AD-A265 166

NTATION PAGE

Form Approved
OMB No. 0704-0188

1. AGENCY USE ONLY (Leave blank)	2. REPORT DATE	3. REPORT TYPE AND DATES COVERED
	April 1993	professional paper

4. TITLE AND SUBTITLE
SPIN-PEIERLS GROUND STATES AND FRUSTRATION IN A MULTI-BAND PEIERLS-HUBBARD MODEL

5. FUNDING NUMBERS
In-house funding

6. AUTHOR(S)
H. Roder, A. R. Bishop, and J. T. Gamel

7. PERFORMING ORGANIZATION NAME(S) AND ADDRESS(ES)
Naval Command, Control and Ocean Surveillance Center (NCCOSC)
RDT&E Division
San Diego, CA 92152-5001

8. PERFORMING ORGANIZATION REPORT NUMBER

9. SPONSORING/MONITORING AGENCY NAME(S) AND ADDRESS(ES)
Naval Command, Control and Ocean Surveillance Center (NCCOSC)
RDT&E Division
San Diego, CA 92152-5001

10. SPONSORING/MONITORING AGENCY REPORT NUMBER

11. SUPPLEMENTARY NOTES

12a. DISTRIBUTION/AVAILABILITY STATEMENT
Approved for public release; distribution is unlimited.

12b. DISTRIBUTION CODE

13. ABSTRACT *(Maximum 200 words)*

We discuss the consequences of including both electron-phonon and electron-electron couplings in multi-band models, focusing on numerical studies of a one-dimensional two-band model in the intermediate regime for both coupling strengths. Spin-Peierls as well as long-period, frustrated ground states are identified, reminiscent of those found in antiferromagnetic next-nearest neighbor (ANNNI) models. We speculate on experimentally observable signatures of this rich phase diagram.

93-12275

Published in *Bulletin of the American Physical Society*, Vol. 37, No. 1.

14. SUBJECT TERMS	15. NUMBER OF PAGES
electron-electron couplings multiband and multiorbital models high-temperature superconductors	16. PRICE CODE

17. SECURITY CLASSIFICATION OF REPORT	18. SECURITY CLASSIFICATION OF THIS PAGE	19. SECURITY CLASSIFICATION OF ABSTRACT	20. LIMITATION OF ABSTRACT
UNCLASSIFIED	UNCLASSIFIED	UNCLASSIFIED	SAME AS REPORT

21a. NAME OF RESPONSIBLE INDIVIDUAL	21b. TELEPHONE (Include Area Code)	21c. OFFICE SYMBOL
J. T. Gammel	(619) 553-6576	Code 573

Spin-Peierls ground states and frustration in a multi-band Peierls-Hubbard model

H. Röder[a], A.R. Bishop[b], and J. Tinka Gammel[c]

[a] *Physikalishes Institüt, Universität Bayreuth, W-8580 Bayreuth, F.R.G.*

[b] *Theoretical Division, Los Alamos National Laboratory, Los Alamos, New Mexico 87545*

[c] *Materials Research Branch, NCCOSC RDT&E Division (NRaD), San Diego, CA 92152-5000*

We discuss the consequences of including both electron-phonon and electron-electron couplings in multi-band models, focusing on numerical studies of a one-dimensional two-band model in the intermediate regime for both coupling strengths. Spin-Peierls as well as long-period, frustrated ground states are identified, reminisent of those found in antiferromagnetic next-nearest neighbor (ANNNI) models. We speculate on experimentally observable signatures of this rich phase diagram.

1992 PACS: 75.30.Fv, 71.45.Lr, 71.38+i, 64.70.Rh

Multi-band and multi-orbital models have recently been much studied, primarily due to their relevance for high-temperature superconductors (HTC) [1]. At stoichiometry, such models can exhibit interesting and unusual ground states, such as electron-phonon (*e*-ph) driven incommensurate long-period (LP) or superlattice (SL) phases [2]. Here we show that a one-dimensional (1D), two-band (2B) model with competing electron-electron (*e*-*e*) and *e*-ph interactions also exhibits at stoichiometry interesting *magnetic* behavior: namely, LP frustrated or spin-Peierls (SP) phases in the intermediate regime between the strongly electron-electron (*e*-*e*) correlated antiferromagnetic (AF) limit and the strongly *e*-ph correlated large lattice distortion (LD) limit. Similar complex LP phases are found in antiferromagnetic next-nearest neighbor (ANNNI) models with competing magnetic interactions [3]. Doping into such SP phases may induce unusual pairing mechanisms in 1D or in the 2D version of this model, relevant to HTC [4-7].

Considerable effort has gone into solving effective one-band (1B) models. For dominant *e*-*e* interactions Zhang and Rice [4] derived in the context of HTC, due to the separation of energy scales, an effective 1B t-J Hamiltonian using a Wannier singlet basis. Imada [7] has suggested that inclusion of an *e*-ph dependence of the effective spin interaction J is crucial, as it leads to the opening of a spin gap, important for singlet superconductivity. Here, we stress phenonena for which keeping the *full* 2B model with *both* *e*-*e* and *e*-ph interactions is essential. These effects are generic in the sense that their existence is not dependent on the exact analytic form of the couplings or the specific parameters used.

We study the 1D, 2B, 3/4-filled, tight-binding Peierls-Hubbard Hamiltonian (PHH) developed [8, 9] to model an interesting class of 1D compounds – halogen-bridged transition-metal linear chain complexes (MX chains) – which exhibit tunable behavior ranging from antiferromagnetic (AF) or spin-density-wave (SDW) to charge-density-wave (CDW) to semimetallic. This same model can be considered as: a model of CuO chains or a 1D analog of the models used for CuO_2 planes in oxide superconductors [10]; a 3/4-filled analog of the the organic conductor polyacetylene; a model for charge-transfer salts such as TTF-TCNQ; or a model of neutral-ionic transitions [11]. If one considers the two orbitals to be on the same site, this Hamiltonian is also related to the Kondo Hamiltonian used to describe heavy fermion and other valence fluctuation materials. This model yields *quantitative* fits for the MX chain compounds to a variety of experimental data (optical absorption, Raman spectra, susceptibility data, ESR, *etc.*) [8, 9]. Unusual magnetic behavior in strong magnetic fields has also been reported in one MX system [12], which may be experimental support for the phenomena discussed here.

Our model 1D, 2B, PHH is [8, 9]:

$$H = \sum_{l,\sigma}\Big\{\left(-t_0+\alpha\delta_l\right)\left(c^\dagger_{l,\sigma}c_{l+1,\sigma}+c^\dagger_{l+1,\sigma}c_{l,\sigma}\right) + \left[\epsilon_l-\beta_l(\delta_l+\delta_{l-1})\right]c^\dagger_{l,\sigma}c_{l,\sigma}\Big\} + \sum_l\Big\{U_l n_{l\uparrow}n_{l\downarrow}+\frac{1}{2}K(\delta_l-a_1)^2+P\delta_l\Big\}, \tag{1}$$

where $c^\dagger_{l,\sigma}$ ($c_{l,\sigma}$) creates (annihilates) an electron at site l with spin σ, and M (d_{z^2}) and X (p_z) Wannier orbitals are situated on even and odd sites, respectively. Each M_2X_2 unit cell has 6 electrons, or 3/4-filling. No non-bonding orbitals were included in the 1D Hamiltonian, and effective springs were used to model these and other such elements of the structure not explicitly included [13]. Parameters are: the on-site energy (electron affinity) ϵ_l ($\epsilon_M=-\epsilon_X=e_0$), electron hopping ($t_0$), on-site ($\beta_M,\beta_X$) and inter-site ($\alpha$) *e*-ph coupling, and on-site (U_M,U_X) *e*-*e* repulsion. a_1 is the natural length of the

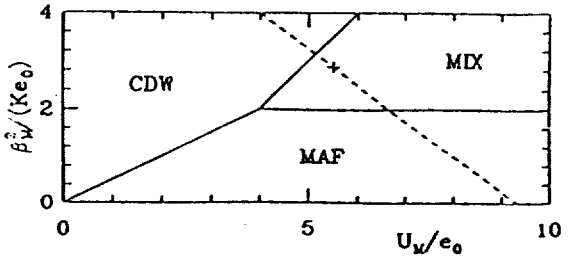

FIG. 1. t_0=0 phase diagram of an infinite chain for β_X/β_M=−1, U_X/U_M=1. The dashed line is the parameter path used for Fig. 4 and + the point in Fig. 3. Note that changing P is equivalent to moving along a line through the origin.

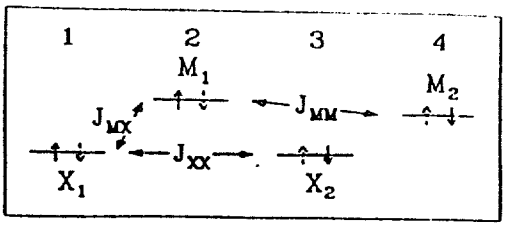

FIG. 2. Schematic energy level diagram in the strongly correlated limit showing frustration of the effective antiferromagnetic couplings due to the partial real-space occupancy of the low-lying levels induced by MX hybridization.

M-X spring K, and δ_l is the relative displacement of the atoms on an N site chain at sites l and l+1. δ_l is determined (self-consistently) by minimizing the total energy E_T, $\partial E_T/\partial\delta_l$=0. The change in average MX bond length a, $a=\sum_l \delta_l/N$, and the pressure P are related by $\partial E_T/\partial P=Na$, yielding $P=K(a_1-a+D)$ where $D=\sum_{l,\sigma}\langle 2\beta_l n_{l,\sigma}-\alpha(c^\dagger_{l,\sigma}c_{l+1,\sigma}+c^\dagger_{l+1,\sigma}c_{l,\sigma})\rangle/NK$. We work at fixed a. We have used both mean-field (Hartree-Fock) and exact diagonalization to study this model [8]. Upon doping, the multi-band nature is manifested in localized intrinsic defects – expected on the basis of effective 1B models [15] to be electron/hole symmetric and chargeless, spinless, and/or distortionless – which exhibit electron/hole asymmetry [14] and local charge, spin, and/or LD character [8,9]: for example local LD around "magnetic" polarons in an AF such as NiCl or NiBr [9]. Near phase boundaries, even at low defect concentration, modification of the background (stoichiometric "ground state") can also occur [16].

Tuning e_0, t_0, U_M, and U_X is essentially a 1D analog of theoretical discussions in 2D which focus on the p-d hybridization in HTC materials. There, as here, these parameters determine the broken symmetry (if any) of the ground state, and the nature of electron or hole doping into those states. Indeed, the similarity is even stronger because the nominal filling at stoichiometry is essentially the same in both MX and oxide HTC materials – 3/4-filling of 2 bands and 5/6-filling of 3 bands, respectively. Furthermore, both AF and CDW HTC compounds exist (*e.g.*, $LaCu_2O_4$, $BaBiO_3$), much as for MX compounds (*e.g.*, NiCl, PtCl, respectively). We stress the MX *class* has the advantage of essentially continuous tunability between these extremes. Finally, even in the context of AF-based HTC materials the role of e-ph coupling is increasingly appreciated [1], where, upon doping, the same local competition of AF and CDW as in MX compounds occurs and can induce strong *local* LD in a strongly magnetic background [6], as observed in doping and photodoping spectroscopy [17].

In the CDW case with large LD, typical of many MX chains, a first approximation is to approach the material as decoupled X=M=X trimers and M monomers. Indeed, optical absorptions in PtCl chains are very close to the monomers and trimers in solution [18]. Similar decoupled-cluster limits can be formulated for the other LD phases, though the analysis does not add significantly to the understanding from the analytic U=0 limit [8] and

TABLE I. The a=a_1=0 constant volume period-4 phases, occupancies, distortions, energies, and effective antiferromagnetic spin correlations J in the $t_0\to 0$ limit. Here $t=t_0/e_0$, $u_{m,x}=U_{M,X}/e_0$, $b_{m,x}=\beta_{M,X}/\sqrt{Ke_0}$, and $\delta(l)\sqrt{K/e_0}=d_X(\cos\frac{l\pi}{2}-\sin\frac{l\pi}{2})-d_M(\cos\frac{l\pi}{2}+\sin\frac{l\pi}{2})$ defines dimensionless $X(M)$ sublattice distortion order parameters $d_X(d_M)$.

phase	$XMXM$	d_M	d_X	$D\sqrt{\frac{K}{e_0}}$	$2E_T/(e_0N)$	$J^{\rm eff}/e_0$
MAF	$\mathbb{1}-\uparrow-\mathbb{1}-\downarrow-$	0	0	$2b_x+b_m$	u_x-1	$\frac{J_{MM}}{e_0}=\frac{t^4(4u_m-u_x+4)}{2u_m(u_m-u_x+2)^2(2u_m-u_x+4)}$
XAF	$\uparrow-\mathbb{1}-\downarrow-\mathbb{1}-$	0	0	b_x+2b_m	u_m+1	$\frac{J_{XX}}{e_0}=\frac{t^4(4u_x-u_m-4)}{2u_x(u_x-u_m-2)^2(2u_x-u_m-4)}$
MIX	$\uparrow=\downarrow-\mathbb{1}\cdots\mathbb{1}-$	$\frac{1}{2}b_m$	$\frac{1}{2}b_x$	$3\frac{b_x+b_m}{2}$	$\frac{u_x+u_m}{2}-\frac{b_x^2+b_m^2}{4}$	$\frac{J_{MX}}{e_0}=\frac{t^2(u_m+u_x)}{(u_x-2+b_x^2-b_m^2)(u_m+2-b_x^2+b_m^2)}$
CDW	$\mathbb{1}=\bullet=\mathbb{1}-\mathbb{1}-$	b_m	0	$2b_x+b_m$	$u_x+\frac{1}{2}u_m-1-b_m^2$	
BOW	$\bullet=\mathbb{1}-\mathbb{1}-\mathbb{1}=$	0	b_x	b_x+2b_m	$\frac{1}{2}u_x+u_m+1-b_x^2$	

A-1

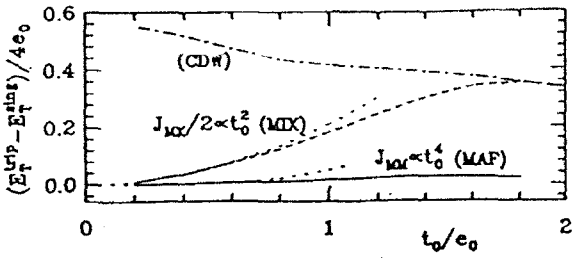

FIG. 3. t_0 dependence of the difference in singlet and triplet energies for the CDW, MIX, and MAF phases at the point indicated by the + in Fig. 1, obtained by exact diagonalization of an N=16 site system. For small t_0, this corresponds to excitations of the effective spin-Hamiltonian $H = 4JS_i^z S_{i+j}^z$ with energy $4J_{MM}$ in the MAF phase and $2J_{MX}$ in the MIX phase, whereas in the CDW phase this reflects the Peierls gap. The dotted lines are the perturbative expressions for J_{MM}, J_{MX} from Table I.

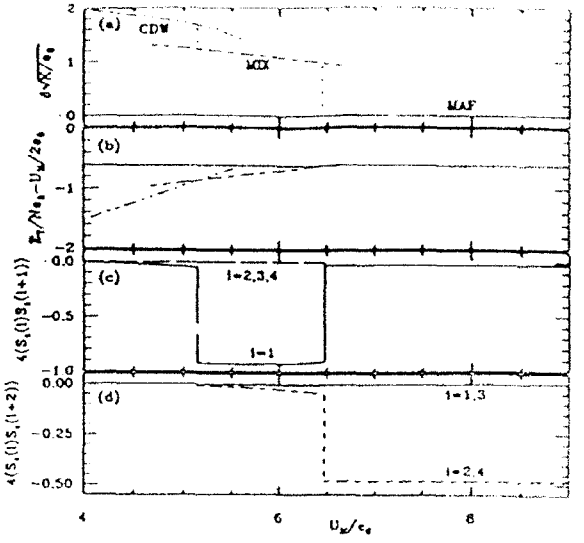

FIG. 4. Exact diagonalization: (a) lattice distortion amplitude, (b) total energy E_T, and (c) n.n. and (d) n.n.n. spin correlations as a function of U_M/e_0 for t_0/e_0=0.5 and N=16 for MAF, CDW, and MIX phases. Other parameters are as in Fig. 1. The charge densities have essentially the t_0=0 values shown schematically in Table I.

t_0=0 limit (described below).

For large (positive) e_0, a reasonable starting point for interpreting the effects of including e-e and e-ph couplings is an effective 1/2-filled, 1B model focusing on the M d_{z^2} orbitals [15]. For zero e-e correlations, when on-site e-ph coupling (β) dominates, the ground state exhibits X-sublattice LD with an accompanying CDW on the M-sublattice (CDW phase). When the intersite e-ph coupling, $\alpha_{1B}^{eff}=\alpha t_0/(2e_0)$, dominates, the case is reversed: X-CDW and M-LD (bond-order-wave (BOW) phase). Typical e-ph phenomena (phonon softening, solitons, *etc.*) are found [15]. The full 2B model leads to qualitative modifications such as removal of the BOW phase [8], and electron-hole asymmetry of defect absorptions [14]. Our focus here is on intermediate to large e-e correlations (large U_M), where in the 1D, 1B limit one expects a SP phase with an effective AF coupling between M sites [4, 5, 19].

To understand the consequences of e-e correlations for a multiband model, we first examine the zero-hopping limit. The period-4 (P4) phases for t_0=α=0 are listed in Table I. The phase diagram for parameter values near the CDW/AF crossover (relevant to MI or NiX materials), is shown in Fig. 1. The phase diagram is more complex for $U_X, |\beta_X| \gtrsim U_M, |\beta_M|$ and/or $\beta_X/\beta_M > 0$, where the hybridization-driven competition is most effective. When t_0=0, all spin excitations are isoenergetic. For $t_0 \neq 0$, AF correlations develop and one can treat the problem in terms of an effective spin model. Without coupling between the two bands, the lower, X-like (for $e_0>0$) band is full and non-magnetic, while the upper, M-like band is 1/2-full with one electron per M site (when e-e repulsion is dominant). The on-site e-ph coupling β leads to a splitting of the upper band which competes with an AF ordering of the spins caused by the effective AF coupling between neighboring metal sites, J_{MM} (as in the effective 1B case). When hybridization between the two bands is allow[illegible]ne lower band is not completely full, and now there [illegible] effective AF coupling between neighboring halide [illegible]s, J_{XX} (dominant when U_X is dominant), as well as M and X sites, J_{MX}. J_{XX} and J_{MX} are not present in 1B models [20]. In fact, when the splitting due to the e-ph coupling β is on the order of U and e_0, the AF state with neighboring M-X pairs singly occupied can become the ground state, as shown in Fig. 1. This implies, in contrast to the 1B case, that the combination of e-e and e-ph coupling in the 2B model drives, in addition to the non-magnetic CDW and BOW phases, three (competing) SP phases: one on the X-sublattice (XAF), one on the M-sublattice (MAF), and one involving MX pairs and large LD (MIX). Since J_{MM}, J_{XX}, and J_{MX} are all AF couplings ($J > 0$), they obviously cannot all be simultaneously satisfied and the system is frustrated, as shown in Fig. 2. It is straightforward to derive from fourth-order perturbation theory in t_0 an effective t, J_{MX}, J_{MM}, J_{XX} model in the large U limit; the resultant J's are listed in Table I. When only one of the J's dominates, one can numerically check this estimate by comparing the energies of the singlet and triplet ground states (at fixed LD). Fig. 3 shows good agreement for small t_0. Note that the CDW phase has an entirely e-ph driven AF component: even when the $X(M)$-LD is large, some residual $M(X)$-sublattice magnetization remains.

For parameters where the LD is large and driven by the on-site e-ph coupling β, and/or the Hubbard U terms are large, the zero-hopping phase diagram is close to the

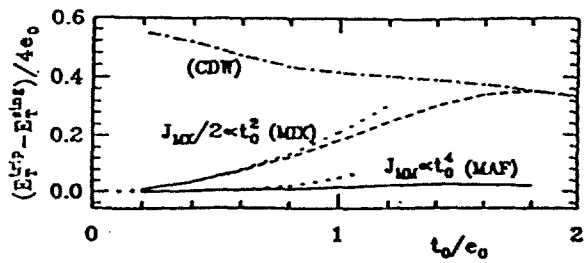

FIG. 3. t_0 dependence of the difference in singlet and triplet energies for the CDW, MIX, and MAF phases at the point indicated by the + in Fig. 1, obtained by exact diagonalization of an N=16 site system. For small t_0, this corresponds to excitations of the effective spin-Hamiltonian $H = 4JS_i^zS_{i+j}^z$ with energy $4J_{MM}$ in the MAF phase and $2J_{MX}$ in the MIX phase, whereas in the CDW phase this reflects the Peierls gap. The dotted lines are the perturbative expressions for J_{MM},J_{MX} from Table I.

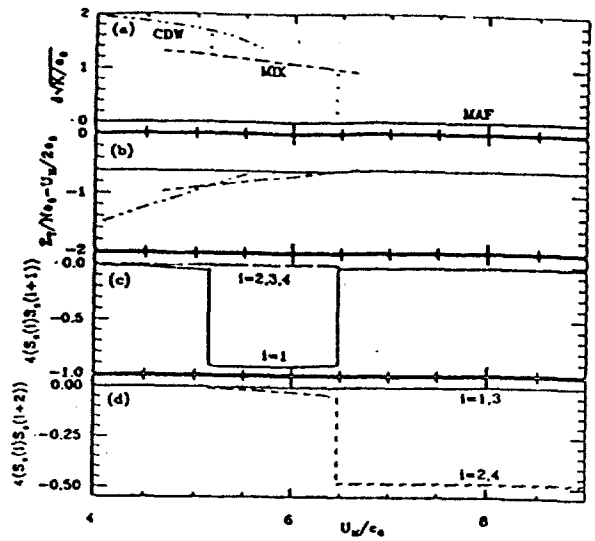

FIG. 4. Exact diagonalization: (a) lattice distortion amplitude, (b) total energy E_T, and (c) n.n. and (d) n.n.n. spin correlations as a function of U_M/e_0 for t_0/e_0=0.5 and N=16 for MAF, CDW, and MIX phases. Other parameters are as in Fig. 1. The charge densities have essentially the t_0=0 values shown schematically in Table I.

t_0=0 limit (described below).

For large (positive) e_0, a reasonable starting point for interpreting the effects of including e-e and e-ph couplings is an effective 1/2-filled, 1B model focusing on the M d_{z^2} orbitals [15]. For zero e-e correlations, when on-site e-ph coupling (β) dominates, the ground state exhibits X-sublattice LD with an accompanying CDW on the M-sublattice (CDW phase). When the intersite e-ph coupling, $\alpha_{1B}^{eff}=\alpha t_0/(2e_0)$, dominates, the case is reversed: X-CDW and M-LD (bond-order-wave (BOW) phase). Typical e-ph phenomena (phonon softening, solitons, *etc.*) are found [15]. The full 2B model leads to qualitative modifications such as removal of the BOW phase [8], and electron-hole asymmetry of defect absorptions [14]. Our focus here is on intermediate to large e-e correlations (large U_M), where in the 1D, 1B limit one expects a SP phase with an effective AF coupling between M sites [4,5,19].

To understand the consequences of e-e correlations for a multiband model, we first examine the zero-hopping limit. The period-4 (P4) phases for t_0=α=0 are listed in Table I. The phase diagram for parameter values near the CDW/AF crossover (relevant to MI or NiX materials), is shown in Fig. 1. The phase diagram is more complex for U_X,$|\beta_X|\gtrsim U_M$,$|\beta_M|$ and/or $\beta_X/\beta_M>0$, where the hybridization-driven competition is most effective. When $t_0\equiv$0, all spin excitations are isoenergetic. For $t_0\neq$0, AF correlations develop and one can treat the problem in terms of an effective spin model. Without coupling between the two bands, the lower, X-like (for e_0>0) band is full and non-magnetic, while the upper, M-like band is 1/2-full with one electron per M site (when e-e repulsion is dominant). The on-site e-ph coupling β leads to a splitting of the upper band which competes with an AF ordering of the spins caused by the effective AF coupling between neighboring metal sites, J_{MM} (as in the effective 1B case). When hybridization between the two bands is allow he lower band is not completely full, and now there 1 effective AF coupling between neighboring halide s, J_{XX} (dominant when U_X is dominant), as well as M and X sites, J_{MX}. J_{XX} and J_{MX} are not present in 1B models [20]. In fact, when the splitting due to the e-ph coupling β is on the order of U and e_0, the AF state with neighboring M-X pairs singly occupied can become the ground state, as shown in Fig. 1. This implies, in contrast to the 1B case, that the combination of e-e and e-ph coupling in the 2B model drives, in addition to the non-magnetic CDW and BOW phases, three (competing) SP phases: one on the X-sublattice (XAF), one on the M-sublattice (MAF), and one involving MX pairs and large LD (MIX). Since J_{MM}, J_{XX}, and J_{MX} are all AF couplings ($J>0$), they obviously cannot all be simultaneously satisfied and the system is frustrated, as shown in Fig. 2. It is straightforward to derive from fourth-order perturbation theory in t_0 an effective t, J_{MX}, J_{MM}, J_{XX} model in the large U limit; the resultant J's are listed in Table I. When only one of the J's dominates, one can numerically check this estimate by comparing the energies of the singlet and triplet ground states (at fixed LD). Fig. 3 shows good agreement for small t_0. Note that the CDW phase has an entirely e-ph driven AF component: even when the $X(M)$-LD is large, some residual $M(X)$-sublattice magnetization remains.

For parameters where the LD is large and driven by the on-site e-ph coupling β, and/or the Hubbard U terms are large, the zero-hopping phase diagram is close to the

actual phase diagram. In Fig. 4 we show the LD, total energy, and spin correlations obtained by exact diagonalization on a ring of 16 sites as parameters are varied along the line shown in Fig. 1. As U_M increases (LD decreases), we observe a sharp transition from M-M charge coupling (CDW) to M-X spin coupling (MIX) to M-M spin coupling (MAF), in agreement with the t_0=0 results. (Since for finite systems the phases are strongly pinned by the LD, we can follow competing phases across phase boundaries.) For larger t_0, the couplings change more smoothly, and charge disproportionation, M-X spin coupling, and M-M spin coupling coexist, with the phase of the LD passing from CDW through MIX to BOW as the amplitude goes to zero. For large t_0, even for U_M=0, the CDW phase shows a strong tendency towards AF order, driven by valence fluctuations rather than U.

The crossover from P4 CDW to P4 MAF is accompanied by LP SL phases [21] when $|\beta_X/\beta_M|>1$, or when the *intersite* e-ph coupling α is large. We have completed only preliminary evaluation of the LP region of the phase diagram, as the many competing metastable states significantly complicate the analysis. An α-driven SL phase has recently been found in a 2D, 3B model of HTC CuO_2 layers [6]. Such SLs may be viewed as an ordered array of discommensuration defects with respect to a nearby commensurate order (*e.g.*, P4). In view of the effective J's discussed above, it may be natural to model such states in terms of ANNNI-like models [3,5,7], where nearest and longer range couplings compete, leading to frustration and associated complexity phenomena – multitimescale relaxation, hysteresis, metastability, *etc.* In the context of the MX class, it will be particularly interesting to investigate materials in, or near, this crossover regime – *e.g.*, PtI – and to further control the crossover with pressure, magnetic field, doping, impurities, *etc.* Indeed *doping* into this complex regime should be highly sensitive to the softness and competitions of the phases: this is an excellent regime to study pairing tendencies and metallization.

In conclusion, we stress that the 1D, 2B, PHH is representative of a very large variety of low-D electronic materials. This variety is mirrored in the model's richness, not only in terms of the potential ground states as discussed here, but also in terms of the consequences of doping into such phases, especially near phase boundaries, where besides the usual plethora of doping and photoinduced non-linear excitations (solitons, polarons, bipolarons, and excitons [8,9,11,15]), a dopant-induced transition of the *global* phase may exist [16,17] and novel pairing mechanisms are anticipated [4–7]. Inclusion of e-ph in a 2D 3B model relevant to HTC materials leads to similar effects both at stoichiometry and upon doping, where generalized polaronic or "bag" states with local coexistence of spin and charge are found [6]. We are attempting to exploit this richness via a systematic "making-measuring-modeling" approach on to the MX class of 1D compounds, which are realizations of this Hamiltonian spanning the range of complex broken symmetry ground states. The recent device proposals for photovoltaics, *etc.*, [22] serve to underscore the exciting consequences of this richness. We believe that experimental investigations of the template [23] and pressure dependence and high (magnetic) field behavior of pure and doped MX materials in the LD/AF cross-over regime, such as PtI, NiBr, or their mixed-metal or -halide analogs, will continue to yield interesting insights into the nature of intrinsically multiband effects and the competition between e-e and e-ph interactions.

Acknowledgements We thank with X.Z. Huang, A. Saxena, J. Shi, and K. Yonemitsu, for important discussions, and E.Y. Loh, Jr. for computational assistance. ARB was supported by the US DOE, HR by the Deutsche Forschungsgemeinschaft through SFB 213, and JTG by a National Research Council-NRaD Research Associateship through a grant from the ONR. Supercomputer access was through the Advanced Computing Laboratory at LANL. HR and JTG are grateful to the hospitality of LANL, where this work was begun.

---

[1] Proceedings of the Conference on Lattice effects in High T_c Superconductors, Sante Fe, NM, 13-15 January, 1992 (World Scientific, in press).
[2] I. Batistić, J.T. Gammel and A.R. Bishop, Phys. Rev. B 44, 13228 (1991).
[3] W. Selke and M.E. Fisher, Phys. Rev. B 20, 257 (1979); P. Bak and J. v. Bohm, Phys. Rev. B 21, 5297 (1980).
[4] F.C. Zhang and T.M. Rice, Phys. Rev. B 37, 3759 (1988); 41, 2560 (1990).
[5] V.J. Emery and G. Reiter, Phys. Rev. B 38, 11938 (1988); 41, 7247 (1990).
[6] K. Yonemitsu *et al.*, unpublished and in Ref. [1].
[7] M. Imada, J. Phys. Soc. Japan 60, 1877 (1991); 61, 423 (1992); unpublished.
[8] J.T. Gammel *et al.*, Phys. Rev. B 45, 6408 (1992);
[9] S.M. Weber-Milbrodt *et al.*, Phys. Rev. B 45, 6435 (1992).
[10] J.T. Gammel *et al.*, Physica B 163, 456 (1990).
[11] A. Painelli and A. Girlando, Synth. Metals 29, F181 (1989); J. Huang *et al.*, unpublished.
[12] M. Haruki and P. Wachter, Phys. Rev. B 43, 6273 (1991).
[13] Longer-range Coulomb effects have been investigated [11]. The e-ph couplings α and β may be viewed as expansions of longer-range Fröhlich-like terms. We have also tested further neighbor hoppings and springs. Such extensions do not change the qualitative discussion here.
[14] J.T. Gammel *et al.*, Phys. Rev. B 42, 10566 (1990).
[15] D. Baeriswyl and A.R. Bishop, Physica Scripta T19, 239 (1987); K. Nasu, J. Phys. Soc. Japan 50, 235 (1981).
[16] J. Reichl, unpublished; S. Marianer, unpublished.
[17] *e.g.*, G.Yu *et al.*, Phys. Rev. Lett. 67, 2581 (1991); G.A. Thomas *et al.*, Phys. Rev. Lett. 67, 2906 (1991).
[18] R. Donohoe, private communication.

[19] J. Shi, R. Bruinsma, and A.R. Bishop, preprint.
[20] While effective 1B t-J models may be valid in both the MAF and MIX phases – *e.g.* using MX singlets [4] potentially with an e-ph dependent J [7] – to model the MAF/MIX crossover would require distinguishing between MX=2↑ and ↑2, and thus a multiorbital model, as at the crossover one can no longer argue there is a separation of energy scales.
[21] Intermediate phases can be driven by the competitions between t_0, β, α, long-range Coulomb fields, and/or the effective short range J's. Such intermediate phases can be P4, as expected from commensurability effects, or LP, since frustration can drive effective long-range interactions, as seen in ANNNI models [3]. The large-β LP phase discussed in Ref. [2], though related, is somewhat different than the frustration driven, magnetic LP phase discussed here or, in 2D, in Ref. [6] (for large α).
[22] L.A. Worl *et al.*, J. Phys. C, in press; A. Saxena *et al.*, Synth. Metals, in press.
[23] In mixed MXX' crystals, the MX' phase may be controlled by the lattice constant of the host MX crystal.

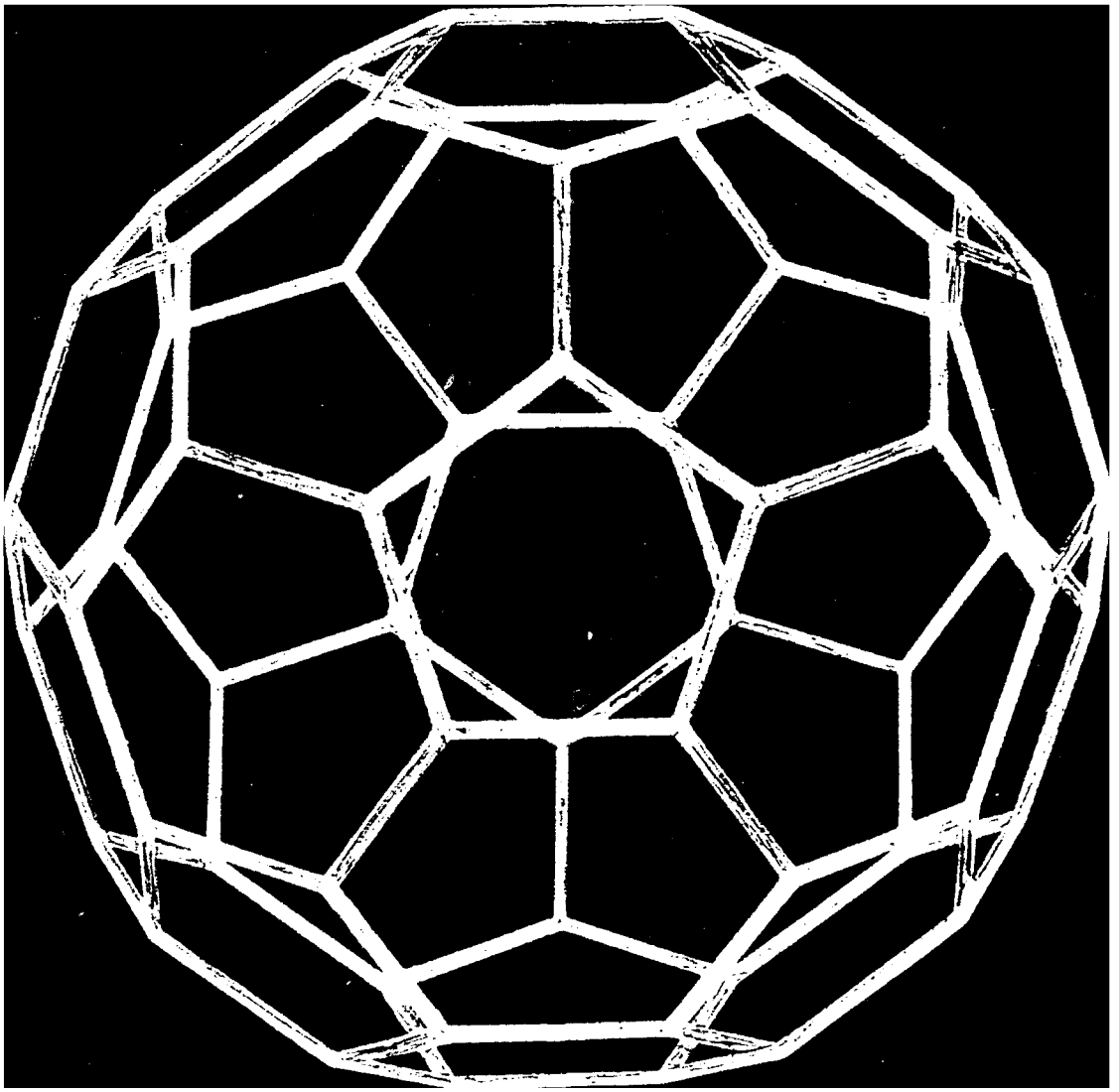

12:12

J15 7 Ground State and Excitations of the Extended Hubbard Model. E.GAGLIANO, S.BACCI AND RICHARD M.MARTIN Univ. of Illinois, Urbana-Champaign.- Using exact diagonalization techniques we study the 1D and 2D Hubbard model with first-neighbor Coulomb interaction, V. The ground state energies as well as static and dynamic correlations are calculated as functions of the local interaction U, V and doping concentration. We will discuss the phase diagram of the model in the (U,V) plane, which beside the CDW-SDW transition at half-filling, has a broad region where phase separation take place. We will analyze also, the effect of V in the superconducting properties of the model.

12:24

J15 8 Monte-Carlo Simulations of an Extended Hubbard Model.* C. S. WANG and ANIKET BHATTACHARYA, University of Maryland.--A three-band extended Hubbard model in the two-dimensional CuO_2 plane has been suggested to contain the essential features of high temperature superconductivity. The phases of the hopping integrals between nearest-neighbor copper-oxygen sites, t_{pd}, and that between nearest-neighbor oxygen-oxygen sites, t_{pp}, are often approximated to yield the same signs for all hopping integrals. Monte-Carlo simulations indicate a rather sudden phase separation with holes localized either on copper or oxygen sites, when $|t_{pp}| \cong |t_{pd}|$. Such a drastic separation would not occur if the appropriate phases of the hopping integrals were taken into account. Instead, the densities on copper and oxygen sites become smooth functions of t_{pp}.

*Supported by NSF (grants No. DMR-8901453).

12:36

J15 9 The Phase Diagram of Doped Oxide Superconductors, the role of direct p-p hopping. Peter S. Riseborough, Polytechnic University. --- A phase diagram for the electron and hole doped high temperature Oxide superconductors is calculated, using a realistic tight binding model for the electronic states in the Copper-Oxide planes. The effect of the coulomb interactions between the electrons in the Copper d shells is accounted for, in the mean field approximation, using the slave boson technique. The effect of the direct hopping of electrons between the p orbitals on nearest neighboring Oxygen ions has a dramatic effect on the metal-insulator phase boundary. A strong asymmetry between the electron and hole doped systems is predicted. This asymmetry may be inferred from experimental data which yields measures of the quasiparticle effective mass.

12:48

J15 10 Cluster Calculations of mid-gap states in high Tc Superconductors A. SAUL, Division Fisica del Solido, Departamento de Fisica, CNEA, Av. del Libertador 8250, 1429 Buenos Aires ARGENTINA, and M. WEISSMANN, Departamento de Fisica de la Materia Condensada C-XII, Universidad Autonoma de Madrid, Cantoblanco, 28049 Madrid ESPANA.-- We have performed semiempirical electronic structure calculations for CuO clusters with different charge and cluster geometry, with 4, 5 and 6 oxygens nearest neighbors of the copper atom. We find a charge transfer gap of 2eV in the three cases, for the stechiometric charges, but levels inside the gap appear with doping. For the planar cluster (CuO_4) they appear with electron doping and are mostly of copper character but for clusters with apical oxygens they appear only with hole doping and are mostly of apical oxygen character. This has suggested a model of an alloy made up of doped and undoped clusters that is useful to explain recent photoemision and soft X-ray absorption experiments. This model also suggest a relation between Tc and the properly normalized dopant concentration.

13:00

J15 11 Structure of Quasiparticles in the t-J, Kondo-Heisenberg and Three-Band Models. G. REITER and O. F. de Alcantara BONFIM, University of Houston --- We construct the solution of the Schrödinger equation for a single hole in an antiferromagnet that corresponds to the lowest order self consistent approximation for the quasiparticle propagator with the background treated in the spin wave approximation (Kane, Lee and Read, Schmitt-Rink, Varma and Ruckenstein). The results are used to compare the background spin configuration around the moving hole in the t-J, Kondo-Heisenberg and Three-Band models. The asymptotic form of the spin deviation is dipolar for the t-J model, as predicted by Shraiman and Siggia, but not for the other models. The spin on the oxygen is not zero, and varies with the wavevector in the lowest band in the Three-Band and Kondo-Heisenberg models.

* This work was partially supported by Grant No. MDA 972-88-G-0002 from U. S. Defense Advanced Research Projects Agency and the State of Texas at the Texas Center for Superconductivity.

13:12

J15 12 Quasiparticle Energies in a Two-Band, Interlayer Coupling Model for a High-T_c Superconductor. W.A. RAINE and W.N. MATHEWS Jr., Georgetown U.--- Much of the recent literature on the high-T_c, layered, cuprate superconductors emphasizes the necessity of including both oxygen and copper bands and, more recently, interlayer correlations, in theoretical models of these materials. Accordingly, we construct a Hamiltonian that takes into account these requirements, and we use this Hamiltonian, together with existing decoupling methods and extensions thereof, to calculate the superconducting state quasiparticle energies. Our result is a generalization, that contains corrections due to the interlayer parameters, of the quasiparticle energies for the corresponding equivalent one-layer model. These corrections also indicate the presence of two superconductor gaps, a result that is in agreement with recent findings. Coupled equations for the energy gaps and hole concentrations in each band can be obtained and solved self-consistently, which provides a starting point for investigating the existence of gap anisotropy in these materials.

13:24

J15 13 CHARGE INSTABILITIES DUE TO ELECTRON-PHONON COUPLING IN THE SINGLE-BAND HOLSTEIN-HUBBARD THEORY FOR CUPRATE SUPERCONDUCTORS A. J. FEDRO, MSD, Argonne National Laboratory (*), and J. ZHONG and H.-B. SCHÜTTLER, Center for Simulational Physics, University of Georgia (+).-- From a multiple band (MB) Hubbard model, we derive the effective single-band (SB) linear electron-phonon (EP) couplings of the correlated 2D CuO_2 conduction electron system to the displacements of in-plane and out-of plane oxygen atoms. We identify the relevant competing groundstate phases, associated with an EP-driven charge instability, in the zero bandwidth ($t=0$) limit and predict a novel, dopant-induced, coexistent charge density wave (CDW) and spin density wave (SDW) ordered state near $\frac{1}{4}$-filling with a CDW $\sqrt{2}\times\sqrt{2}$- and a SDW 2×2-supercell, respectively. We show that, as a consequence of the Franck-Condon principle, even a very strong EP coupling will have only a negligibly small effect on the observable electronic and spin excitations in the undoped, insulating groundstate phase of the cuprates.

(*) Supported by U.S.D.O.E., BES-Materials Sciences, Contract No. W-31-109-ENG-38.

(+) Supported by the National Science Foundation under Grant No DMR-8913878 and by the University of Georgia Office of the Vice President for Research.

13:36

J15 14 Spin-Peierls Ground States and Frustration in a Multi-Band Peierls-Hubbard Model J. TINKA GAMMEL, *Naval Ocean Systems Center*, H. RÖDER, *Universität Bayreuth*, and A.R. BISHOP, *Los Alamos National Laboratory*.

We discuss the consequences of including both electron-phonon and electron-electron couplings in multi band models

After briefly discussing two analytic limits — the large Hubbard U (antiferromagnetic) limit and the strongly distorted (bond- or charge-density-wave) limit — we focus on (exact) numerical studies of a one-dimensional two-band model, developed for halogen bridged transition metal linear chain complexes (MX chains), using parameter values in the intermediate regime for both the electron-electron and electron-phonon couplings, where unusual spin-Peierls or long-period, frustrated ground states are found, similar to those in ANNNI models. We speculate on possible experimentally observable signatures of this rich phase diagram.

* Work at UB partially supported by SFB213, and work at LANL supported by the US DOE. JTG is currently supported by a NRC-NOSC Research Associateship

SESSION J16: HTSC: LOCAL ATOMIC STRUCTURE
Wednesday morning, 18 March 1992; Room 144 at 11:00; T. Egami, presiding

Invited Paper

11:00

J16 1 Internal Structural Models of Superconductive Cluster Compounds.
KARIN M. RABE, Yale University.

Both Chevrel compounds, $M_yMo_6Ch_{8-x}O_x$(M = Sn, Pb, Eu, Cu,...; Ch = S, Se, Te), and A_xC_{60} (A = K, Rb, Cs) contain anionic metallic clusters weakly coupled by metallic cations. Chemical and structural trends in these materials reveal many anomalies which the present model, motivated by the observed proximity of high-T_c superconductivity to pressure and compositional phase boundaries and low temperature lattice instabilities, explains for the first time. In this model, there is a stress-driven phase separation on intermediate length scales into a well-crystallized primary phase and a poorly ordered second phase or array of extended defects stabilized by the presence of the primary phase. If this second phase is electronically distinct, profound effects on the properties of the material may result. In Chevrel compounds, formation of a semiconducting second phase, related to the low temperature rhombohedral-triclinic lattice instability and the effect of substitutional oxygen defects and associated large local strains on crystal structure and T_c, can account for anomalies in the pressure dependence of T_c and transport properties in the superconducting and normal states[1]. In doped C_{60}, the second phase forms a connected high-T_c superconductive matrix, marginally stabilized by fcc crystallites[2]. In general, the second phases need not support the coherent scattering necessary for detection through x-ray diffraction experiments. Rather, their presence must be inferred from observed chemical trends in structure, stability and properties.

[1]J. C. Phillips and K. M. Rabe, submitted to Europhysics Letters.
[2]K. M. Rabe, J. C. Phillips and J. M. Vandenberg, to be published in Physical Review B.

Contributed Papers

11:36

J16 2 Structural Phase Transitions in Doped and Undoped La_2CuO_4. M.K. CRAWFORD, R.L. HARLOW, E.M. MCCARRON and W.E. FARNETH, DuPont, J.D. AXE and H. CHOU, Brookhaven National Laboratory, Q. HUANG, National Institute of Standards and Technology. --- La_2CuO_4 exists in several structural modifications which are related by CuO_6 octahedra rotations about the (110) or (1$\bar{1}$0) axes of the high temperature I4/mmm phase. We have used[1] synchrotron x-ray and neutron diffraction to study phase transitions involving such octahedra rotations in La_2CuO_4 samples which have isovalent and/or aliovalent substitutions at the La^{3+} site. These structural transformations profoundly effect superconductivity for reasons which are not completely understood. Furthermore, there is some evidence for a commensurate electronic or magnetic instability at a doping level of 1/8 hole per Cu atom in these systems. We will discuss these issues in light of our recent experimental results.

[1] M.K. Crawford et al., Phys. Rev. B 44, 7749 (1991).

11:48

J16 3 Local Atomic Structure of Strontium and Neodymium Doped Lanthanum Cooper Oxides. T. R. Sendyka, T. Egami, Univ. of Pennsylvania, M. K. Crawford, E. M. McCarron, du Pont de Nemours. --- The local atomic structure of $La_{1.85}Nd_{0.2}Sr_{0.15}CuO_4$, and $La_{1.85}Nd_{0.6}Sr_{0.15}CuO_4$ was studied by pair distribution function (PDF) analysis of the neutron powder diffraction data, taken at the SEPD station at IPNS. Even though the average structure is the same, local atomic structure is found to be different from the ideal La_2CuO_4 structure. The shifts in atomic positions are in the order of up to 0.1 Å. The deviation is temperature dependent. For the Nd.6 composition distribution in the interatomic O-O distances exhibits a change near 60K. The observed structural changes are related to the LTT - LTO phase transition which is known to affect superconductivity. Differences in the local structure of those two phases will be discussed. Work at the Univ. of Pennsylvania was supported by NSF through grant DMR 90-01704.

12:00

J16 4 Anomalous X-Ray Scattering Study of $La_{1.85}Sr_{0.15}Cu_{1-x-y}Ni_xZn_yO_4$. S. N. EHRLICH, M. A. CASTRO, S. A. HOFFMAN and S. M. DURBIN, Purdue Univ. - Anomalous x-ray scattering measurements were made on $La_{1.85}Sr_{0.15}CuO_4$, a 40 K superconductor, with and without dopants of magnetic Ni and non-magnetic Zn in order to determine the dopant site occupancy distribution. We are investigating the effects of dopants on T_c which appear to be sensitive to the magnetic character of the impurity. In order to interpret changes in T_c in these samples it is necessary to know what sites the Ni and Zn atoms occupy in the lattice structure. We measured the intensities of several reflections, and also did fluorescence EXAFS measurements, for each sample at energies below and above the K absorption edge of Ni, Cu and Zn. The EXAFS measurements were used to calculate the structure factor for each of the above elements as a function of energy. The site distributions of these elements is determined by fitting the measured intensity data to the intensities calculated